HHS Public Access

Author manuscript

Dev Cell. Author manuscript; available in PMC 2023 December 05.

Published in final edited form as:

Dev Cell. 2022 December 05; 57(23): 2652–2660.e3. doi:10.1016/j.devcel.2022.11.003.

Mouse placenta fetal macrophages arise from endothelial cells outside the placenta

Xiaowen Chen[1], **Alan T. Tang**[1], **Joanna Tober**[2], **Jisheng Yang**[1], **N. Adrian Leu**[3], **Stephanie Sterling**[3], **Mei Chen**[1], **Yiqing Yang**[1], **Patricia Mericko-Ishizuka**[1], **Nancy A. Speck**[2], **Mark L. Kahn**[1,4,*]

[1]Cardiovascular Institute and Department of Medicine, Perelman School of Medicine, University of Pennsylvania, Philadelphia, Pennsylvania, USA 19104

[2]Department of Cell and Developmental Biology, Perelman School of Medicine, University of Pennsylvania, Philadelphia, Pennsylvania, USA 19104

[3]Transgenic Mouse Core, School of Veterinary Medicine, University of Pennsylvania, Philadelphia, Pennsylvania, USA 19104

[4]Lead contact

Abstract

Placental fetal macrophages (fMacs) are the only immune cells on the fetal side of the placental barrier. Mouse models have not been used to test their function as they have previously been found to have distinct cellular origins and functions in mice and humans. Here we test the ontogeny of mouse placental fMacs. Using a new Hoxa13^{Cre} allele that labels all placental endothelial cells (ECs) we demonstrate that mouse placenta fMacs do not arise from placental endothelium. Instead, lineage tracing studies using Tie2-Cre and Cx3cr1^{CreERT2} alleles demonstrate mouse placental fMacs arise from yolk sac endothelium. Administration of blocking antibodies against CSF1R at E6.5 and E7.5 results in depletion of placental fMacs throughout pregnancy, suggesting a yolk sac origin, similar to human fMacs. This Matters Arising paper is in response to Liang et al. (2021), published in Developmental Cell. A response by Liang and Liu (2022) is published in this issue.

In Brief (eTOC blurb)

In this Matters Arising article, Chen et al. use a newly generated Hoxa13^{Cre} allele to show mouse placenta fetal macrophages (fMacs) originate from placenta endothelium, differing from the origin

*Corresponding author: Dr. Mark L. Kahn, markkahn@pennmedicine.upenn.edu.

AUTHOR CONTRIBUTIONS

Conceptualization, XC and MLK; investigation, XC, ATT, JT, JY, AL, SS, MC, YY and PM; supervision, MLK; writing-original draft, XC; writing-review & editing, XC, NAS and MLK.

DECLARATION OF INTERESTS

The authors declare no competing interests.

described in Liang et al (2021). They demonstrate that fMacs are yolk sac with similar origin to human Hofbauer cells.

Graphical Abstract

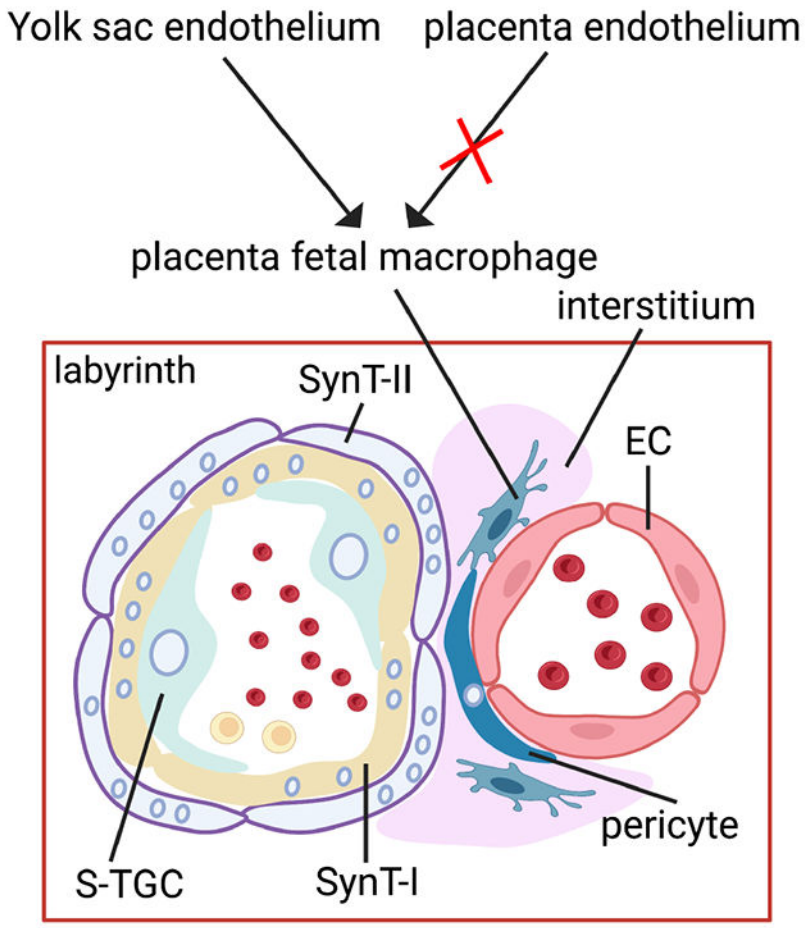

INTRODUCTION

The mammalian placenta is a transient organ that transfers nutrients, gases and waste across the feto-maternal border and secretes factors that control maternal cardiovascular and immune function during pregnancy[1]. During gestation the placenta also provides an immunological barrier between the mother and fetus that is believed to be essential for successful pregnancy[2]. In addition to the trophoblast lined channels that carry maternal blood and the fetal vascular network that forms next to those channels, tissue macrophages invest both the maternal and fetal side of the placenta. Maternal macrophages found in the decidua and intervillous space arise from maternal circulating monocytes[3]. Placental fMacs, known as Hofbauer cells (HBCs) in the human placenta, are the only fetus-derived immune cells found in the placenta and are implicated in protecting the fetus from maternal infection and immune responses and in formation of the fetal blood vasculature in the placenta[4].

However, functional studies have not yet been performed to test and better define the role of these macrophages in vivo.

Human HBCs appear at an early timepoint during placentation, 18 days post conception, and are found in the interstitial space within the placental villi, the vascular exchange units of the human placenta where endothelial-lined vessels carrying fetal blood come in close contact with trophoblast-lined vessels carrying maternal blood[5]. HBCs have recently been characterized in detail using scRNA-Seq and flow cytometry and found to closely resemble yolk sac-derived TRMs[6]. The mouse and human placenta are both hemochorial (i.e. maternal blood runs through fetal trophoblast lined channels), and in vivo mouse models and in vitro-derived murine trophoblast stem cells have been valuable research tools for understanding human placental development and function[7,8]. However, the use of the mouse to investigate placenta fMacs in vivo has been recently discouraged by a study published in *Developmental Cell* reporting that mouse placental fMacs arise from placental ECs through a process of endothelial-hematopoietic transition (EHT)[9]. As a consequence of the presumed difference in origin and anatomic location between human and mouse placental fMacs, it has been proposed that mouse is not an appropriate or valuable model for studying HBC biology and function[5].

In the present study we apply genetic lineage tracing strategies using both new and existing Cre-expressing mouse lines to demonstrate that mouse placenta fMacs do not arise from placental ECs, but are instead yolk sac derived TRMs that invade the placenta early in gestation. Consistent with these results, mouse placenta fMacs can be ablated using antibodies to CSF1R at timepoints during early pregnancy. These studies demonstrate that mouse placental fMacs closely resemble human HBCs in terms of location and ontogeny, and lay the foundation for future functional studies to better define their roles in placental development and maternal-fetal immunity.

Results

Mouse placental fMacs accumulate around fetal vessels in the labyrinth after E10.5

The structure of the mouse placenta and a typical fetal-maternal circulation unit-labyrinth is shown in Figure 1A. To better characterize the time of detection and location of mouse placental fMacs, we performed immunostaining of E9.5, E10.5, E11.5, E13.5 and E17.5 mouse placenta sections using anti-F4/80 and anti-CD45 antibodies. CD45 marks all leukocytes, and F4/80 is a marker of mature macrophages, including HBCs (placental fMacs)[10,11]. Immunostaining revealed round $CD45^{+}F4/80^{-}$ maternal hematopoietic cells (mHCs) in maternal blood within trophoblast lined channels (Figure 1B, right) and $CD45^{+}F4/80^{+}$ irregular and elongated cells in the extravascular space on the fetal side of the placenta (Figure 1B, left). At E9.5 a small number of $F4/80^{+}CD45^{+}$ macrophages could be detected in the yolk sac, but not in the placenta (Supplemental Figure 1). In the placenta $F4/80^{+}CD45^{+}$ fMacs were first detected at E10.5 and E11.5 in the chorioallantoic region closest to the embryo proper, and were later detected in the adjacent vascular labyrinth region farther from the embryo proper (Figure 1C, white arrows). After E11.5 these cells were found in increasing numbers in the labyrinth region throughout the duration of gestation (Figure 1D).

Anti-F4/80 staining and co-staining with antibodies to detect SynT-I cells (type I syncytiotrophoblasts) (anti-MCT1), SynT-II cells (type II syncytiotrophoblasts) (anti-MCT4), ECs (anti-Endomucin) and a reporter expressing R26-LSL-TdTomato (Ai14) to detect cells expressing a $Pdgfrb^{CreERT2}$ knockin allele that expresses specifically in pericytes was used to determine the precise spatial localization of fMacs in the mouse placenta. Placental fMacs were located in the perivascular space that lies between ECs and Syn T-II cells in the labyrinth (Figure 1E–G), a space also occupied by pericytes. Placental fMacs in the chorioallantoic region were detected in the interstitum, frequently adjacent to the large vessels that bridge the labyrinth with the umbilical vessels (Figure 1C, left panels). These studies suggest that mouse placenta fMacs appear at a timepoint after yolk sac fMacs, and are frequently located in close association with placental fetal vasculature.

To determine if placental fMacs undergo local proliferation, we stained placenta sections at E10.5, E11.5, E13.5 and E17.5 with antibodies to F4/80 and the cell division marker Ki67. Ki67 staining revealed a high proliferative rate at E10.5 (50-60% Ki67-positive) that steadily declined throughout gestation (Figure 1H–1I). This pattern was reciprocal to that observed for total cell numbers (Figure 1D), suggesting that placental fMacs arrive at an early timepoint and expand rapidly during early-mid gestation. These findings support a mechanism of local proliferation rather than recruitment from circulating monocytes or other sources during gestation (addressed further below).

Hoxa13^{Cre} lineage tracing demonstrates that placental endothelium does not give rise to placenta fMacs.

Placental ECs arise independently from the allantois, an extraembryonic mesodermal derivative[12]. The *Hoxa13* gene is expressed in the allantois starting at E7.5 and its expression extinguished by E9.5[13,14]. In the embryo proper *Hoxa13* is expressed in the developing limbs but not in vascular ECs or their precursors[13]. Thus, the pattern of endogenous *Hoxa13* expression suggests that it would be an ideal tool with which to identify placental cells that arise from the allantoic lineages such as placental endothelium. Prior studies using gene targeting of the *Hoxa13* locus to express Cre recombinase have confirmed that placental ECs arise from allantoic *Hoxa13*$^{+}$ precursors, but since these alleles only labeled approximately 40% of placental ECs[9,13], they are not suitable for functional gene deletion studies and have limited sensitivity for allantoic lineage tracing studies. Using a new Hoxa13Cre knockin line, Liang et al has recently concluded that mouse placental fMacs arise in the placenta from hemogenic placental ECs, and thus have origins that appear distinct from human HBCs[5,9].

To define allantois-derived cells we used gene targeting in embryonic stem (ES) cells to introduce a T2A-Cre fusion gene at the end of the Hoxa13 coding region in exon 2 (Figure 2A). Prior to creating the final $Hoxa13^{Cre}$ allele used for these studies, we generated a $Hoxa13^{Cre\text{-}WPRE}$ knockin allele that included a similar 3' WPRE-polyA cassette used by Liang et al[9] that is designed to augment Cre expression levels, flanked by FRT sites for in vivo removal with FLPo recombinase if it altered Hoxa13 regulation (Supplemental Figure 2A). Indeed, we found that the $Hoxa13^{Cre\text{-}WPRE}$ allele exhibited Cre activity at numerous sites in the embryo and placenta where endogenous Hoxa13 is not expressed,

including strong expression in the yolk sac where TRMs emerge prior to placental fMacs (Supplemental Figure 2B vs C–E), findings relevant to the discrepancy between our results and those previously reported by Liang et al[9]. Following FLP removal of these exogenous 3' sequences we crossed the Hoxa13^{Cre} allele to R26-LSL-TdTomato (Ai14) reporter mice to define the Hoxa13^{Cre} lineage across the placenta, yolk sac and embryo proper. At E8.5, TdTomato (TdT) expression was detected specifically in the allantois, with no detectable signal in the embryo or yolk sac (Figure 2B). Co-staining of E8.5 uterine and placental tissue sections with Endomucin revealed strong co-localization of ECs with Hoxa13^{Cre} activity in the placenta but not the uterus (Figure 2C). At E11.5, wholemount imaging demonstrated that the placenta and umbilical cord were strongly positive for Ai14 reporter activity (Figure 2D). Reporter activity was also detected in the tail and limb bud of the embryo (white arrows in Figure 2D), consistent with prior studies of Hoxa13 gene expression at those sites[13]. Immunostaining of placenta tissue sections at E11.5, a timepoint at which the placenta is fully functional, demonstrated that virtually all Endomucin^{+} placental ECs were also positive for TdT expressed from the Ai14 reporter gene (Figure 2E–2F). Identical results were obtained when Hoxa13^{Cre} lineage tracing in placenta was performed immunohistochemically using the mTmG reporter that was also utilized by Liang et al [9] (Supplemental Figure 3A, B). Finally, we performed flow cytometry to quantitatively measure the placenta EC labeling efficiency by Hoxa13^{Cre} using mTmG reporter. Using flow cytometry to detect expression of GFP and CD31, approximately 85% of CD31^{+} cells were GFP^{+} (Supplemental Figure 3C, D). The less complete labeling of CD31^{+} cells by flow cytometry compared with the virtually complete labeling using of Endomucin^{+} cells detected by immunostaining of tissue sections may reflect sample contamination with ECs from the maternal decidua or the embryo proper, or the fact that CD31 is also expressed by some trophoblast cells[15]. Significantly, ECs in vascular beds within the embryo proper, including yolk sac, brain and heart, were not labeled by Hoxa13^{Cre} (Figure 2G). Extensive labeling of umbilical cord mesenchymal cells and ECs was detected (Figure 2G), consistent with prior studies indicating that much of those tissues arise from the allantois[16]. Hoxa13^{Cre} lineage tracing also labeled Col1a1-positive placental stromal cells that also arise from the allantois (Figure 2H), although TdT expression was less intense than in placental ECs. These studies demonstrate that the newly generated Hoxa13^{Cre} allele can be used to lineage trace placental ECs from a very early timepoint in their development with high sensitivity.

We next used the Hoxa13^{Cre} allele to test whether mouse placenta fMacs arise from placental ECs as was recently reported[9]. Flow cytometry of cells derived from Hoxa13^{Cre} ;mTmG placentas detected a small number of F4/80^{+} cells that were GFP^{+} (approximately 3%, Supplemental Figure 4A). In contrast, immunostaining for CD45 and F4/80 on E13.5 placental sections from Hoxa13^{Cre} ;Ai14 animals failed to identify any CD45^{+}F4/80^{+} fMacs that were TdT^{+} among more than 1000 examined in the labyrinth and chorioallantoic region (CA) (0 TdT^{+}F4/80^{+} fMacs/1000 F4/80^{+} fMacs measured in four placentas) (Figure 3A, B and D). Thus the 3% of F4/80^{+} cells labeled by Hoxa13^{Cre} activity could not be identified by immunostaining of the placenta. Unlike lineage tracing studies performed using the Hoxa13^{Cre} allele, lineage tracing with the pan-EC driver Tie2-Cre (TEK-Cre) [17] labeled virtually all F4/80^{+}CD45^{+} placental fMacs (588 of 600 fMacs were TdT^{+} in three placentas) (Figure 3C, D). Since Liang et al used CD68 rather than

F4/80 to identify placental fMacs, we also tested whether $CD68^+$ cells were labeled in $Hoxa13^{Cre}$;Ai14 placentas. We found that the punctate CD68 staining overlapped well with F4/80 staining in placental fMacs, and did not identify a distinct F4/80-negative population of macrophages (Supplemental Figure 4B, C). As observed following F4/80 staining, we detected no TdT^+;$CD68^+$ cells among more than 300 examined in the labyrinth and chorioallantoic region (CA) (Supplemental Figure 4B, C). These findings indicated that placental fMacs in the mouse are not derived in situ from placental vasculature, but instead arise from $Tie2^+$ ECs outside the placenta.

Lineage tracing and functional studies identify mouse placental fMacs as yolk sac-derived TRMs.

The finding that placental fMacs appear early in gestation and arise from ECs outside the placenta suggested that they may be TRMs generated in the yolk sac[18]. Prior studies have demonstrated that yolk sac-derived macrophages express CX3CR1 and are efficiently labeled by $Cx3cr1^{CreERT2}$ allele[19]. We therefore next induced $Cx3cr1^{CreERT2}$;Ai14 animals with a single dose of tamoxifen at E9 and examined the placenta at E13.5 (Figure 4A). Immunostaining demonstrated that virtually all $F4/80^+$ placental fMacs were TdT^+ (Figure 4B, C), indicating that they derive from Cx3cr1-expressing yolk sac primitive macrophages.

CSF1R is required for the formation of yolk sac-derived TRMs[20], and past studies have demonstrated that anti-CSF1R antibodies administered maternally early in gestation can block the formation of yolk sac-derived TRMs in the developing embryo[21]. We therefore next tested whether maternal injection of anti-CSF1R antibodies affected mouse placental fMacs. Administration of anti-CSF1R antibody at E6.5 and E7.5, timepoints prior to formation of the placenta, resulted in an approximately 95% reduction in $F4/80^+$ placental fMacs detected by immunostaining of tissue sections at both E13.5 and E17.5 (from 191 to 13 per section at E13.5, and 758 to 34 per section at E17.5) compared with injection of control antibody (Figure 4D, E). The ability of anti-CSF1R antibodies administered at such an early timepoint in gestation to virtually eliminate placental fMacs even at the latest timepoint in gestation indicates that placental fMacs arise from a single pool of progenitors present prior to placentation. Thus, the results of both lineage tracing studies and functional studies support the conclusion that mouse placental fMacs are TRMs that are mainly derived from yolk sac during the whole pregnancy.

Discussion

Our studies refute a previous study showing that placental fMacs are derived from placental hemogenic ECs using a similar $Hoxa13^{Cre}$ knockin allele[9] (and also see the reply to this Matters Arising [22]). While the reasons for these discrepant findings remain speculative, we can propose two likely explanations. First, Liang et al. [9] relied on interpretation of flow cytometry and single cell RNA data that could not unambiguously identify placental fMacs through their characteristic perivascular location in the placenta itself. Using a similar flow cytometric approach we could also identify a small population of $F4/80^+$ cells labeled by $Hoxa13^{Cre}$, but examination of >1000 bona fide placental fMacs in the actual placenta using two distinct markers for those cells (F4/80 and CD68) failed to support these data, and instead suggest that they are false positive events detected in the absence of essential

spatial context. Second, it is possible that the allele generated by Liang et al [9] might express in a leaky, non-endogenous pattern in the embryo because it replaces endogenous 3' regulatory elements with a WPRE-SV40 polyA cassette. Indeed, we found that our independently-generated Hoxa13$^{Cre\text{-}WPRE}$ allele exhibited Cre activity at numerous sites in the embryo and placenta where endogenous Hoxa13 is not expressed, including strong expression in the yolk sac where TRMs emerge (Supplemental Figure 2B vs C–E).

The lineage tracing and functional studies reported in this study identify mouse placental fMacs as TRMs like those that colonize the brain or gonadal tissues[23,24], a result consistent with recent descriptive studies of human HBC gene expression[6]. Although the mouse placenta labyrinth has a more limited interstitial space between the maternal and fetal circulations compared to human placental villi, the two hemochorial placentae share a similar cellular composition in this region (such as fMacs and pericytes). The most important impact of our studies is that they support the conclusion that both the ontogeny and localization of placental fMacs are conserved between mice and humans. TRMs lose many of their functional characteristics when removed from tissues[25], emphasizing the importance of animal models with which to study their biological function. Our studies support the use of pharmacologic and genetic approaches in the mouse to better understand the functional roles of placental fMacs and HBCs during normal and complicated pregnancies.

STAR METHODS

RESOURCE AVAILABILITY

Lead contact—Further information and requests for resources and reagents should be directed to and will be fulfilled by Mark L. Kahn (markkahn@pennmedicine.upenn.edu).

Materials availability—All unique research materials generated in this work will be shared by the lead contact upon reasonable request and under MTA agreement with University of Pennsylvania.

Data and code availability—All data reported in this work will be shared by the lead contact upon reasonable request.

This paper does not report original code.

Any additional information required to reanalyze the data reported in this work is available from the lead contact upon reasonable request.

EXPERIMENTAL MODEL AND SUBJECT DETAILS

Mice—B6.Cg-Gt(ROSA)26Sortm14(CAG-tdTomato)Hze/J (007914), B6.129(Cg)-Gt(ROSA)26Sortm4(ACTB-tdTomato,-EGFP)Luo/J (007676), B6D2F1/J (100006), B6.Cg-Pdgfrbtm1.1(cre/ERT2)Csln/J (030201), B6.Cg-Tg(Tek-cre)1Ywa/J (008863), B6.129P2(C)-Cx3cr1tm2.1(cre/ERT2)Jung/J (020940), and B6.129S4-Gt(ROSA)26Sortm2(FLP*)Sor/J (012930) were obtained from Jackson Laboratories. Hoxa13$^{Cre\text{-}WPRE}$ and Hoxa13^{Cre} mice generated in this study were described below. For

timed matings, embryonic day 0.5 (E0.5) was identified by the time a vaginal plug was discovered. The pregnant dams at the indicated times were sacrificed and the embryo and placenta were dissected out from the uterus. All experiments were performed at least twice using different litters and used littermate controls on a mixed background unless otherwise indicated. These mice were maintained in a specific pathogen-free environment under a 14/10 hour light/dark cycle and all animal experiments described were performed in accordance and approval of the University of Pennsylvania Institutional Animal Care and Use Committee.

METHOD DETAILS

Generation of the Hoxa13^{Cre} knockin allele—ES targeting technology was used to generate the Hoxa13^{Cre} knockin allele as previously described[26]. A targeting construct comprised of 1.5 kb flanking homology arms, T2A-fused Cre coding region, and a flippase recombination target (FRT)–flanked neomycin resistance cassette was synthesized by GenScript. A guide RNA sequence 5′-AACTCAAGACCACTAGTTAA-3′ targeting exon 2 was cloned into the PX330 plasmid (Addgene, 42230) and a corresponding protospacer adjacent motif NGG site was mutated on the targeting construct. V6.5 ES cells were targeted by transfection of targeting construct and PX330 plasmids using XFect for mouse ES cells (Takara, 631320) followed by G418 selection. Individual clones were picked, expanded, and characterized by PCR reactions and Sanger sequencing. Chimeras were produced by microinjection of select ES cells into preimplantation embryos. The male chimeras were bred with B6D2F1/J females to generate F1 germline animals. Genomic DNA PCR was done to screen for germline transmission of the Hoxa13^{Cre} allele using primers (Forward primer: 5’-TGCCTTACACTAAGGTGCAGT-3’; Reverse primer: 5’-CAGGTTCTGCGGGAAACCA-3’). All PCR products were separated on an agarose gel and visualized by SYBR-safe staining. The procedures about ES cell microinjection and manipulation of mouse embryos were done in the Transgenic Mouse Core at Penn Vet as previously described[25]. To generate the final Hoxa13^{Cre} knockin allele used in this manuscript, the above Hoxa13^{Cre} allele mice were further bred with FLPo mice to remove the sequences flanked by FRT sites, which includes neo cassette, exogenous PolyA and WPRE. Hoxa13^{Cre} positive and Flp negative offsprings were selected for general use in the manuscript.

Tamoxifen administration—For Cx3cr1^{CreERT2} tracing, 4 mg Tamoxifen (T5648, Sigma) was dissolved in corn oil and intraperitoneally injected into E9 pregnant dams. For Pdgfrb^{CreERT2} tracing, 5 mg Tamoxifen was orally gavaged into E10.5 pregnant dams.

Yolk sac primitive macrophage depletion assay.—Pregnant dams at E6.5 and E7.5 were intraperitoneally injected with 3 mg rat anti-mouse CSF1R antibody (BE-0213, X-Bio) as previously shown[21]. The control dams at the same age were administrated with 3 mg Rat IgG2a control antibody (BE-0089, X-Bio). The mice at the indicated days of pregnancy were sacrificed and processed at a similar time and manner for placenta and fetus dissection.

Immunostaining of tissue sections.—Embryo, placentae and tissue samples were fixed in 2-4% paraformaldehyde (PFA) in PBS overnight at 4°C with gentle shaking,

gradually dehydrated with 100% ethanol, and embedded in paraffin. Sections of 6-7 μm were prepared for immunostaining. The paraffin sections were deparaffined and incubated with primary antibody diluted in Antibody Diluent pH 7.4 (IW-1000, IHC World). For cryosections, samples were fixed in 2-4% PFA in PBS overnight and submerged in 30% sucrose and then embedded in OCT. Sections of 7-10 μm were collected and stored at −80°C. Cryosections were rehydrated in PBS. The following primary antibodies were used for immunostaining: rabbit anti-RFP (1:200, 600-401-379, Rockland), Goat anti-GFP (1:200, ab6673, Abcam), Rabbit anti-F4/80 (1:100, 70076, CST) (specific for paraffin section), Rat anti-F4/80 (1:200, ab6640, Abcam) (specific for frozen section), Rabbit anti-CD68 (1:200, 97778, CST), Goat anti-Endomucin (1:200, AF4666, R&D), Rat anti-Endomucin (1:100, sc-65495, Santa Cruz), Goat anti-CD45 (1:200, AF114, R&D), Chicken anti-MCT1 (1:200, AB1286-I, Sigma), Rabbit anti-MCT4 (1:200, AB3316P, Sigma) and Rabbit anti-Col1a1 (1:200, 72026, CST). Secondary antibodies were from Thermo Fisher. Control sections were always placed on the same slide, treated and stained under identical conditions. Images were acquired with X4, X10, X20 objectives on a Nikon 80i Eclipse microscope or Leica SP8 Confocal microscope at the same exposure times using NIS Elements Digital Imaging software or Leica LAS X system. ImageJ was used for image processing after data acquisition.

Flow cytometry—mTmG females were mated with Hoxa13^{Cre} males, E11.5 placentas were harvested and decidual tissues were removed. After several washes in cold PBS, the fetal part of the placenta was passed though 20G and 25G needles several times and then digested in DMEM containing collagenase, Dispase and DNase I for 30 min. Standard flow cytometry was followed and the primary antibodies were: PE-CD45, APC-Ter119, BV421-F4/80, APC-CY7-CD31. All antibodies were from BioLegend or BD Biosciences. 7AAD staining was used to exclude dead cells. FACS analysis was performed on a BD LSRII Flow Cytometer at Penn Cytomics and Cell Sorting facility. FACS data were analyzed using FlowJo software.

QUANTIFICATION AND STATISTICAL ANALYSIS

All data were analyzed with GraphPad Prism (version 8). P values were calculated using an unpaired two-tailed Student’s t test or one-way ANOVA plus Tukey post hoc analysis as indicated. P values <0.05 were considered statistically significant and were indicated as follows: *, $P < 0.05$; **, $P < 0.01$; ***, $P < 0.001$; and ****, $P < 0.0001$; ns, not significant.

Supplementary Material

Refer to Web version on PubMed Central for supplementary material.

ACKNOWLEDGEMENTS

We thank members of the Kahn Lab for insightful comments during the course of the work. We are particularly grateful to Michelle Lee for her excellent animal care. Schematic diagram in Figure 1 was created with BioRender.com. This research was supported by an American Heart Association Postdoctoral Fellowship (20POST35200213) to XC and National Institutes of Health R01HL091724 to NAS.

REFERENCES

1. Burton GJ, and Fowden AL (2015). The placenta: A multifaceted, transient organ. Philos. Trans. R. Soc. B Biol. Sci 370. 10.1098/rstb.2014.0066.
2. Ander SE, Diamond MS, and Coyne CB (2019). Immune responses at the maternal-fetal interface. Sci. Immunol 4. 10.1126/sciimmunol.aat6114.
3. Mezouar S, Katsogiannou M, Ben Amara A, Bretelle F, and Mege JL (2021). Placental macrophages: Origin, heterogeneity, function and role in pregnancy-associated infections. Placenta 103. 10.1016/j.placenta.2020.10.017.
4. Zulu MZ, Martinez FO, Gordon S, and Gray CM (2019). The Elusive Role of Placental Macrophages: The Hofbauer Cell. J. Innate Immun 10.1159/000497416.
5. Thomas JR, Naidu P, Appios A, and McGovern N (2021). The Ontogeny and Function of Placental Macrophages. Front. Immunol 12. 10.3389/fimmu.2021.771054.
6. Thomas JR, Appios A, Zhao X, Dutkiewicz R, Donde M, Lee CYC, Naidu P, Lee C, Cerveira J, Liu B, et al. (2020). Phenotypic and functional characterization of first-trimester human placental macrophages, Hofbauer cells. J. Exp. Med 218. 10.1084/JEM.20200891.
7. Hemberger M, Hanna CW, and Dean W (2020). Mechanisms of early placental development in mouse and humans. Nat. Rev. Genet 21. 10.1038/s41576-019-0169-4.
8. Woods L, Perez-Garcia V, and Hemberger M (2018). Regulation of Placental Development and Its Impact on Fetal Growth—New Insights From Mouse Models. Front. Endocrinol. (Lausanne) 9. 10.3389/fendo.2018.00570.
9. Liang G, Zhou C, Jiang X, Zhang Y, Huang B, Gao S, Kang Z, Ma D, Wang F, Gottgens B, et al. (2021). De novo generation of macrophage from placenta-derived hemogenic endothelium. Dev. Cell 56, 2121–2133.e6. 10.1016/j.devcel.2021.06.005. [PubMed: 34197725]
10. Bertrand JY, Jalil A, Klaine M, Jung S, Cumano A, and Godin I (2005). Three pathways to mature macrophages in the early mouse yolk sac. Blood 106, 3004–3011.10.1182/BLOOD-2005-02-0461. [PubMed: 16020514]
11. Takahashi K, Naito M, Katabuchi H, and Higashi K (1991). Development, Differentiation, and Maturation of Macrophages in the Chorionic Villi of Mouse Placenta With Special Reference to the Origin of Hofbauer Cells. J. Leukoc. Biol 50, 57–68. 10.1002/JLB.50.1.57. [PubMed: 2056247]
12. Arora R, and Papaioannou VE (2012). The murine allantois: A model system for the study of blood vessel formation. Blood 120, 2562–2572. 10.1182/blood-2012-03-390070. [PubMed: 22855605]
13. Scotti M, and Kmita M (2012). Recruitment of 5' Hoxa genes in the allantois is essential for proper extra-embryonic function in placental mammals. Development 139, 731–739. 10.1242/dev.075408. [PubMed: 22219351]
14. Shaut CAE, Keene DR, Sorensen LK, Li DY, and Stadler HS (2008). HOXA13 is essential for placental vascular patterning and labyrinth endothelial specification. PLoS Genet. 4. 10.1371/journal.pgen.1000073.
15. Nelson AC, Mould AW, Bikoff EK, and Robertson EJ (2016). Single-cell RNA-seq reveals cell type-specific transcriptional signatures at the maternal-foetal interface during pregnancy. Nat. Commun 7. 10.1038/ncomms11414.
16. Inman KE, and Downs KM (2007). The murine allantois: Emerging paradigms in development of the mammalian umbilical cord and its relation to the fetus. Genesis 45, 237–258. 10.1002/dvg.20281. [PubMed: 17440924]
17. Isermann B, Hendrickson SB, Zogg M, Wing M, Cummiskey M, Kisanuki YY, Yanagisawa M, and Weiler H (2001). Endothelium-specific loss of murine thrombomodulin disrupts the protein C anticoagulant pathway and causes juvenile-onset thrombosis. J. Clin. Invest 108, 537–546. 10.1172/JCI200113077. [PubMed: 11518727]
18. Gomez Perdiguero E, Klapproth K, Schulz C, Busch K, Azzoni E, Crozet L, Garner H, Trouillet C, De Bruijn MF, Geissmann F, et al. (2015). Tissue-resident macrophages originate from yolk-sac-derived erythro-myeloid progenitors. Nature 518, 547–551. 10.1038/nature13989. [PubMed: 25470051]

19. Yona S, Kim KW, Wolf Y, Mildner A, Varol D, Breker M, Strauss-Ayali D, Viukov S, Guilliams M, Misharin A, et al. (2013). Fate Mapping Reveals Origins and Dynamics of Monocytes and Tissue Macrophages under Homeostasis. Immunity 38. 10.1016/j.immuni.2012.12.001.

20. Yosef N, Vadakkan TJ, Park JH, Poché RA, Thomas JL, and Dickinson ME (2018). The phenotypic and functional properties of mouse yolk-sac-derived embryonic macrophages. Dev. Biol 442, 138–154. 10.1016/j.ydbio.2018.07.009. [PubMed: 30016639]

21. Hoeffel G, Chen J, Lavin Y, Low D, Almeida FF, See P, Beaudin AE, Lum J, Low I, Forsberg EC, et al. (2015). C-Myb+ Erythro-Myeloid Progenitor-Derived Fetal Monocytes Give Rise to Adult Tissue-Resident Macrophages. Immunity 42, 665–678. 10.1016/j.immuni.2015.03.011. [PubMed: 25902481]

22. Liang and Liu. A reply to “Mouse placenta fetal macrophages arise from endothelial cells outside the placenta” In this issue of Developmental Cell

23. DeFalco T, Bhattacharya I, Williams AV, Sams DM, and Capel B (2014). Yolk-sac-derived macrophages regulate fetal testis vascularization and morphogenesis. Proc. Natl. Acad. Sci. U. S. A 111. 10.1073/pnas.1400057111.

24. Ginhoux F, Greter M, Leboeuf M, Nandi S, See P, Gokhan S, Mehler MF, Conway SJ, Ng LG, Stanley ER, et al. (2010). Fate mapping analysis reveals that adult microglia derive from primitive macrophages. Science (80-.). 330, 841–845. 10.1126/science.1194637.

25. Roberts AW, Lee BL, Deguine J, John S, Shlomchik MJ, and Barton GM (2017). Tissue-Resident Macrophages Are Locally Programmed for Silent Clearance of Apoptotic Cells. Immunity 47, 913–927.e6. 10.1016/j.immuni.2017.10.006. [PubMed: 29150239]

26. Hong CC, Tang AT, Detter MR, Choi JP, Wang R, Yang X, Guerrero AA, Wittig CF, Hobson N, Girard R, et al. (2020). Cerebral cavernous malformations are driven by ADAMTS5 proteolysis of versican. J. Exp. Med 217. 10.1084/JEM.20200140.

Highlights

1. A new Hoxa13^{Cre} knockin mice specifically target all placenta endothelial cells.
2. Mouse placenta fetal macrophages do not arise from placental endothelium.
3. Mouse placenta fetal macrophages are tissue resident macrophages from the yolk sac.
4. Mouse placental fetal macrophages share a common origin as human Hofbauer cells.

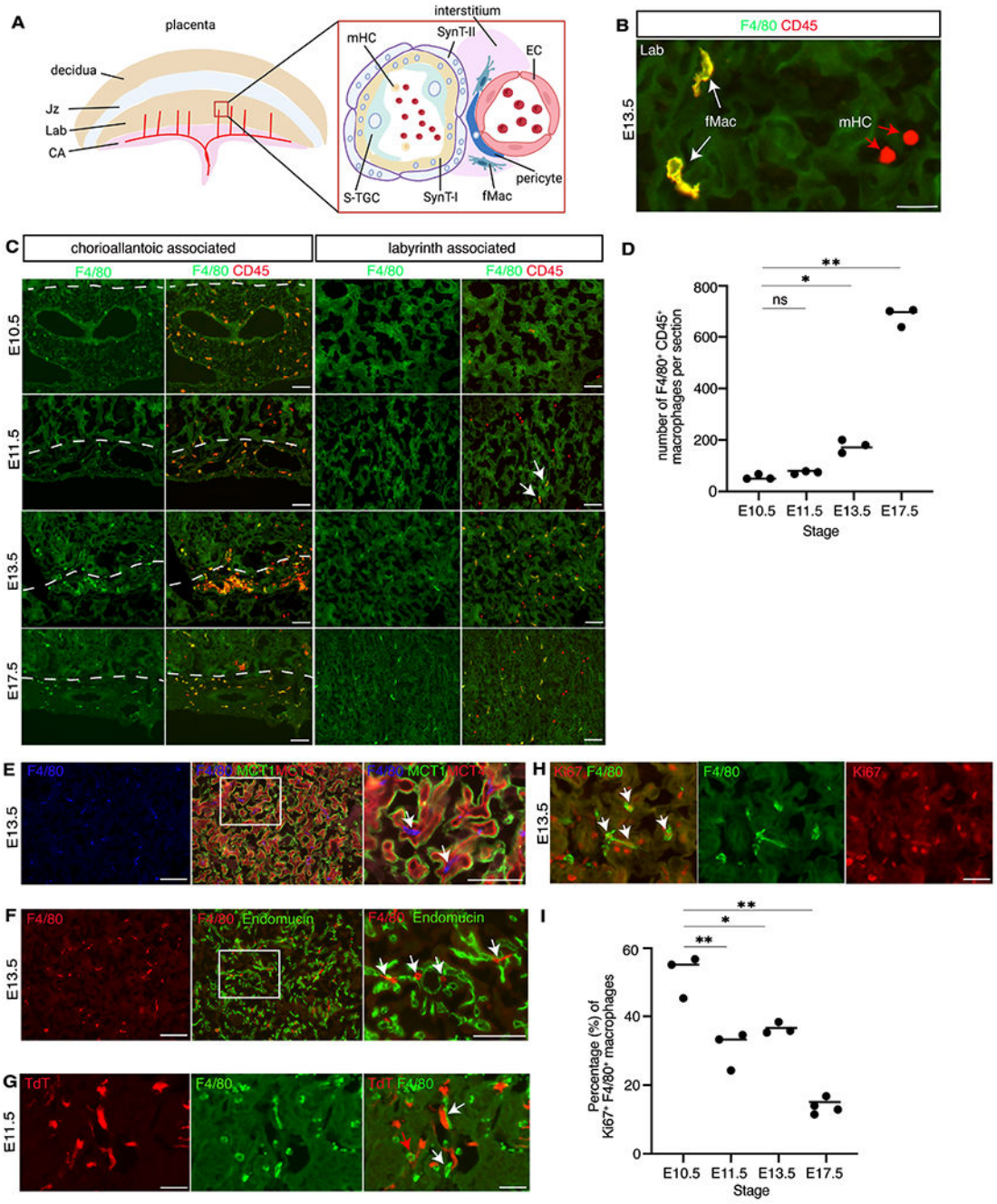

Figure 1. Mouse placental fMacs are located in the perivascular space and expand through local proliferation.

(A) Schematics of the mouse mature placenta (left) and labyrinth (right) are shown. Thin pink lines on the left indicate fetal blood vessels. Jz, junctional zone. Lab, labyrinth. CA, Chorioallantoic region (CA). SynT-I, type I syncytiotrophoblasts. SynT-II, type 2 syncytiotrophoblasts. S-TGC, sinusoidal trophoblast giant cells. mHC, maternal hematopoietic cells. EC, endothelial cell. fMac, fetal macrophage. (B) Immunofluorescence staining for F4/80 (green) and CD45 (red) on wildtype E13.5 placenta sections (N=3). White arrows indicate F4/80^{+}CD45^{+} placental fMacs. Red arrows indicate maternal

hematopoietic cells (mHCs). (C) Immunofluorescence staining for F4/80 (green) and CD45 (red) on wildtype E10.5, E11.5, E13.5 and E17.5 placenta sections (N=3). Left two panels show the chorioallantoic region, while the right two panels show staining in the labyrinth. White arrows indicate $F4/80^{+}CD45^{+}$ macrophages in E11.5 labyrinth. Dotted line indicates boundary between labyrinth and CA. (D) Quantification of $F4/80^{+}CD45^{+}$ placental fetal macrophages detected by immunostaining of placenta tissue sections. Each dot represents the number of detected cells in sections from middle part of one placenta. (E) Immunofluorescence staining for F4/80 (blue) and MCT4 (red) and MCT1 (green) on E13.5 wildtype placenta (N=2). White arrows indicate fetal macrophages. (F) Immunofluorescence staining for Endomucin (green) and F4/80 (red) on E13.5 wildtype placenta sections (N=3). White arrows indicate fetal macrophages. (G) Immunofluorescence staining for F4/80 (green) and TdT (red) on E11.5 $Pdgfrb^{CreERT2}$;Ai14 placenta paraffin sections (N=2). The white arrows indicate fetal macrophages. The red arrow indicates nonspecific blood cell signal. (H) Immunofluorescence staining for F4/80 (green) and Ki67 (red) on E13.5 wildtype placenta sections (N=3). The white arrows indicate $Ki67^{+}$ placental fMacs. (I) Quantification of $Ki67^{+}$ placental fMacs detected using immunostaining for Ki67 and F4/80 on tissue sections. Each dot represents one placenta and three to four sections were examined per placenta. In D and I, *, $p<0.05$; **, $p<0.01$; ns, not significant, Scale bars: 20 μm (B); 10 μm (C-F); 50 μm (G-H).

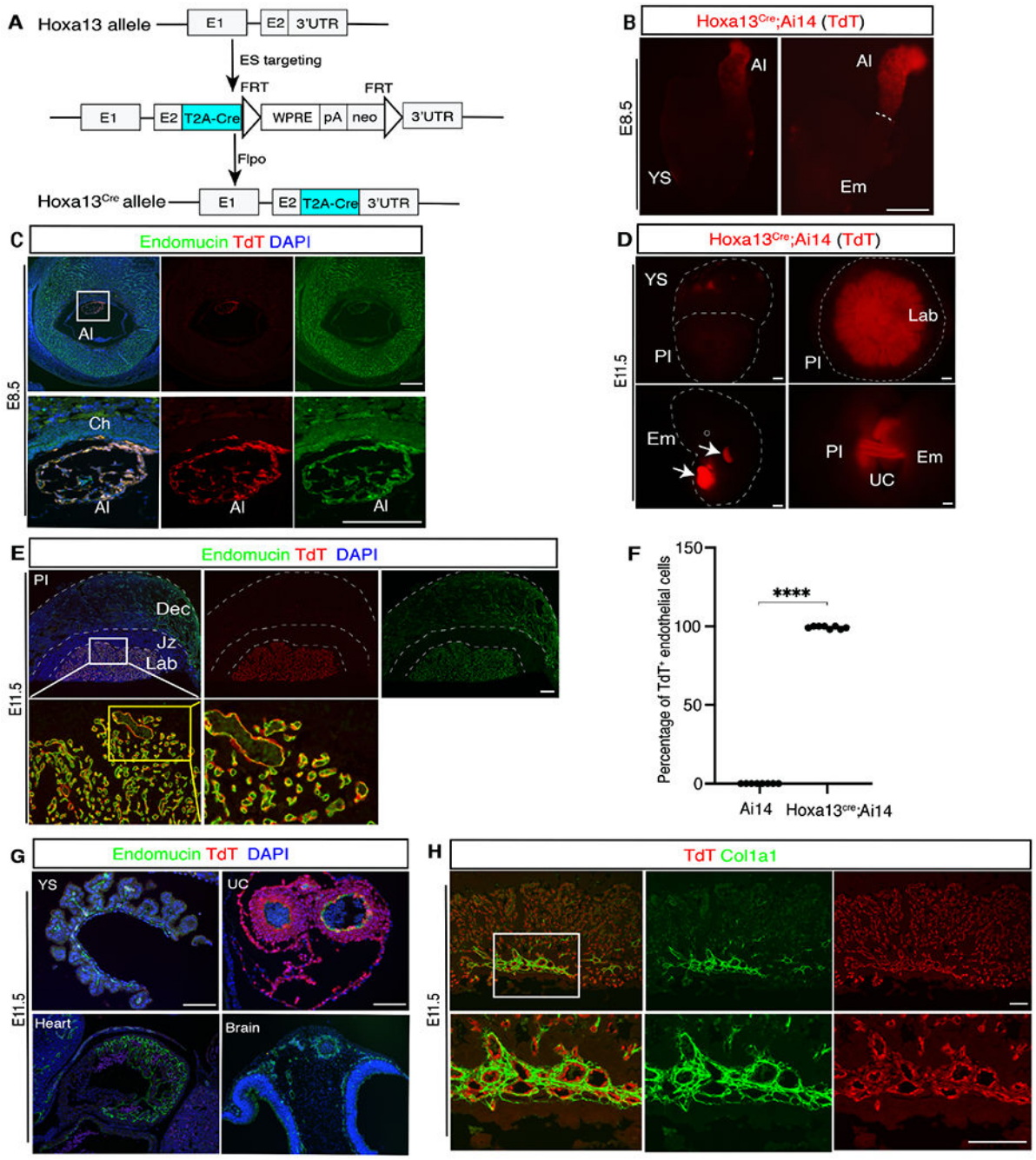

Figure 2. Hoxa13^{Cre} labels ECs in the placenta but not embryo proper.

(A) Generation of the Hoxa13^{Cre} allele. The cyan indicates exogenous elements (T2A-Cre) that were inserted in frame into the Hoxa13 coding sequence in the terminal exon. (B) Fluorescent imaging of TdT activity in freshly harvested Hoxa13^{Cre} ;Ai14 yolk sac (YS), allantois (Al) and embryo (Em) tissues at E8.5. The dotted line indicates the base of the allantois. (C) Immunofluorescence staining for Endomucin (green), TdT (red) and DAPI (blue) on paraffin sections of whole E8.5 Hoxa13^{Cre} ;Ai14 conceptuses (N=3). The boxed area below shows the allantois at higher magnification. Al, allantois; Ch, chorion. (D)

Fluorescent images of E11.5 Hoxa13^{Cre}; Ai14 whole embryo, placenta and umbilical cord (N=3). The dotted lines outline the conceptus, embryo and placenta. YS, yolk sac; Pl, placenta; Lab, labyrinth; Em, embryo; UC, umbilical cord. (E) Immunofluorescence staining for Endomucin (green), TdT (red) and DAPI (blue) on E11.5 Hoxa13^{Cre} ;Ai14 placenta sagittal sections (N=4). The left lower image shows the enlarged image of the white boxed area in the upper panel. The middle lower panel shows the enlarged image of the left lower image. Dec, decidua; Jz, junctional zone; Lab, labyrinth. (F) Quantification of TdT^{+} placental fetal ECs on sections of E11.5 Hoxa13^{Cre} ;Ai14 lineage traced placenta. Each dot represents the % of positive cells identified on three sections from a single placenta. ****, p<0.0001. (G) Immunofluorescence staining for Endomucin (green) and TdT (red) on sections from yolk sac (YS), umbilical cord (UC), heart and brain of E11.5 Hoxa13^{Cre} lineage traced embryo (N=4). (H) Immunofluorescence staining for Col1a1 (green) and TdT (red) on paraffin sections of E11.5 Hoxa13^{Cre} ;Ai14 lineage traced placenta (N=2). The lower panels shows the enlarged images of the boxed area in the upper left panel. Scale bars: 500 μm (B and D); 20 μm (C, E and G); 100 μm (H).

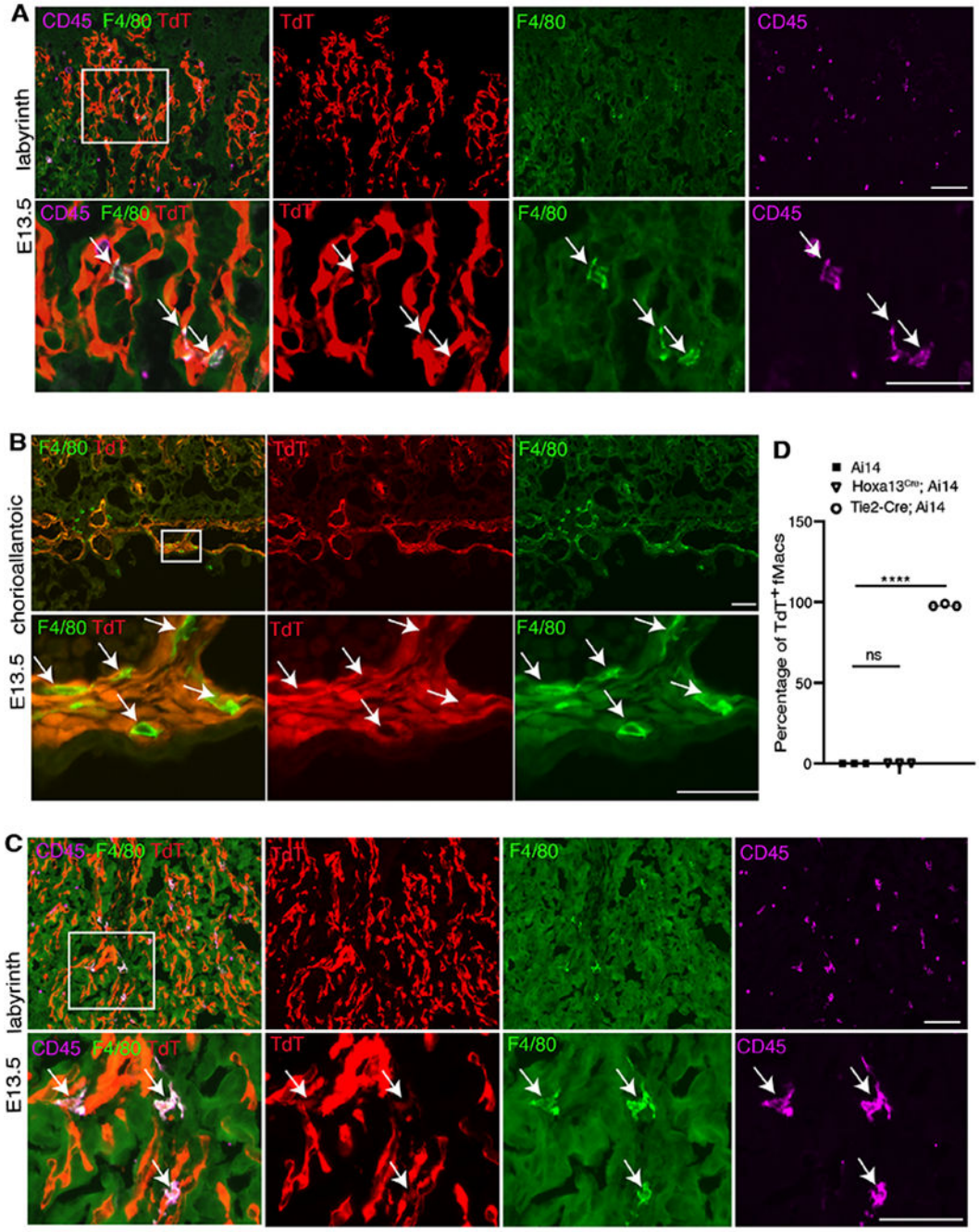

Figure 3. Placental fMacs are derived from extra-placental Tie2^{+} cells.

(A) Immunofluorescence staining for F4/80 (green), CD45 (magenta) and direct fluorescent detection of TdT (red) on frozen sections of E13.5 Hoxa13^{Cre} ;Ai14 lineage traced placental labyrinth (N=3). The lower panels show the enlarged images of the white boxed area indicated in the upper left panel. The white arrows indicate placental fMacs. (B) Immunofluorescence staining for F4/80 (green) and detection of TdT (red) on frozen sections of E13.5 Hoxa13^{Cre}; Ai14 lineage traced placenta chorioallantoic region (N=3). The boxed region above is shown at higher magnification below. White arrows indicate

placenta fMacs. Note F4/80^{+} placenta fMacs are very closely associated with TdT^{+} fetal ECs or stromal cells. (C) Immunofluorescence staining for F4/80 (green), CD45 (magenta) and detection of TdT (red) on frozen sections of E13.5 Tie2-Cre Ai14 lineage traced placenta labyrinth (N=3). The lower panel showed the enlarged images of the white boxed areas in the upper left panel. The white arrows indicate labeling of placental fMacs. Scale bars: 50 μm. (D) Quantification of percentage of TdT^{+} placental fMacs in the above Tie2-Cre and Hoxa13^{Cre} lineage tracing experiments. ****, P<0.001 and ns, not significant.

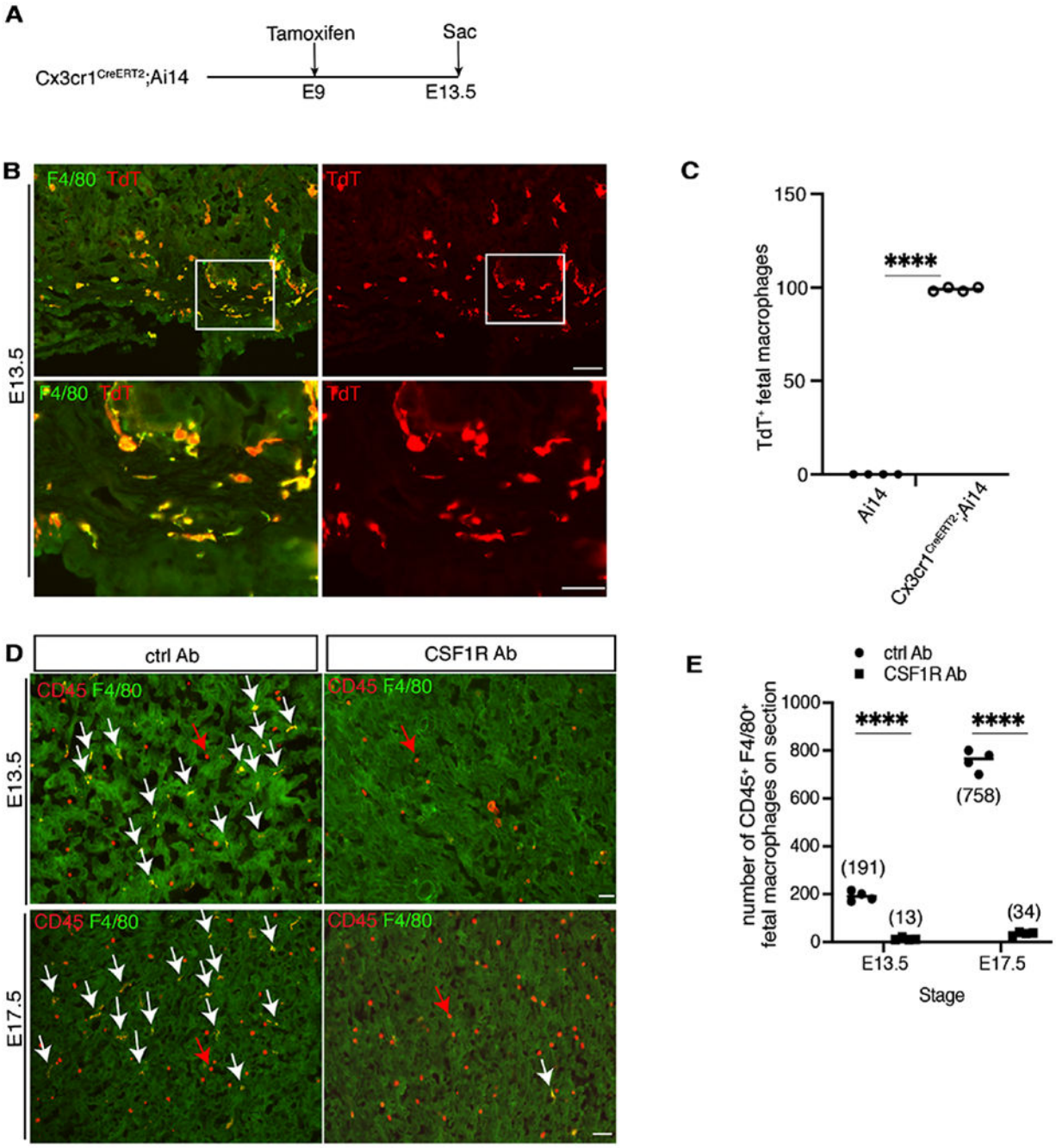

Figure 4. Mouse placental fMacs are lineage traced by Cx3cr1^{CreERT2} and ablated by anti-CSF1R antibodies.

(A) Schematic of Cx3cr1^{CreERT2} lineage tracing using Ai14 reporter. (B) Immunofluorescence staining for F4/80 (green) and detection of TdT (red) on frozen sections of E13.5 Cx3cr1^{CreERT2} lineage traced placenta (N=4). The lower panel shows an enlarged image of the white boxed areas in upper panels. (C) Quantification of Cx3cr1^{CreERT2} ;Ai14 lineage traced F4/80^{+} cells in the E13.5 placenta. Control placenta was Ai14 reporter only. (D) Immunofluorescence staining for F4/80 (green) and CD45 (red) on frozen sections of E13.5 (upper panel) and E17.5 (lower panel) placenta collected from

control antibody (left panel) and CSF1R antibody (right panel) treated dams (N=4). The white arrows indicate F4/80^{+}CD45^{+} placental fMacs. The red arrows indicate examples of F4/80^{-}CD45^{+} maternal hematopoietic cells. (E) Quantification of numbers of F4/80^{+}CD45^{+} placental fMacs in (D). The numbers indicate average number of placental fMacs per section. In C and E, ****, $p<0.0001$. Scale bars: 10 μm.

Key resources table

REAGENT or RESOURCE	SOURCE	IDENTIFIER
Antibodies		
rabbit anti-RFP	Rockland	Cat: 600-401-379
Goat anti-GFP	Abcam	Cat: ab6673
Rabbit anti-F4/80	CST	Cat: 70076
Rat anti-F4/80	Abcam	Cat: ab6640
Rabbit anti-CD68	CST	Cat: 97778
Goat anti-Endomucin	R&D	Cat: AF4666
Rat anti-Endomucin	Santa Cruz	Cat: sc-65495
Goat anti-CD45	R&D	Cat: AF114
Chicken anti-MCT1	Sigma-Millipore	Cat: AB1286-I
Rabbit anti-MCT4	Sigma-Millipore	Cat: AB3316P
Rabbit anti-Col1a1	CST	Cat: 72026
PE-CD45	BioLegend	Cat: 103106
APC-Ter119	BioLegend	Cat: 116212
BV421-F4/80	BD Biosciences	Cat: 565411
APC-CY7-CD31	BioLegend	Cat: 102439
Rat IgG2a control antibody	X-Bio	Cat: BE-0089
Rat anti-CSF1R antibody	X-Bio	Cat: BE-0123
Chemicals, peptides, and recombinant proteins		
Tamoxifen	Sigma	Cat: T5648
Collagenase	Sigma	Cat: C0130-1G
Dispase II	Sigma	Cat: D4693-1G
DNase I	Sigma	Cat: 4716728001
7AAD viability staining solution	BioLegend	Cat: 420404
Experimental Models: cell lines		
mouse ES cells	Takara	Cat: 631320
Experimental models: Organisms/strains		
Mouse: B6.Cg-Gt(ROSA)26Sortm14(CAG-tdTomato)Hze/J	The Jackson Laboratory	JAX: 007914
Mouse: B6.129(Cg)-Gt(ROSA)26Sortm4(ACTB-tdTomato,-EGFP)Luo/J	The Jackson Laboratory	JAX: 007676
Mouse: B6D2F1/J	The Jackson Laboratory	JAX: 100006
Mouse: B6.Cg-Pdgfrbtm1.1(cre/ERT2)Csln/J	The Jackson Laboratory	JAX: 030201
Mouse: B6.Cg-Tg(Tek-cre)1Ywa/J	The Jackson Laboratory	JAX: 008863
B6.129P2(C)-Cx3cr1tm2.1(cre/ERT2)Jung/J	The Jackson Laboratory	JAX: 020940
B6.129S4-Gt(ROSA)26Sortm2(FLP*)Sor/J	The Jackson Laboratory	JAX: 012930

REAGENT or RESOURCE	SOURCE	IDENTIFIER
Hoxa13$^{Cre\text{-}WPRE}$	This paper	N/A
Hoxa13^{Cre}	This paper	N/A
Oligonucleotides		
Hoxa13Cre gRNA sequence: 5′-AACTCAAGACCACTAGTTAA-3′	This paper	N/A
Hoxa13Cre genotyping forward primer: 5′-TGCCTTACACTAAGGTGCAGT-3′	This paper	N/A
Hoxa13Cre genoptying reverse primer: 5′-CAGGTTCTGCGGGAAACCA-3′	This paper	N/A
Recombinant DNA		
Plasmid: Hoxa13^{Cre} ES targeting construct	GenScript	N/A
Plasmid: PX330	Addgene	42230
Software and algorithms		
Adobe Illustrator 2020	Adobe	https://www.adobe.com/
SnapGene	SnapGene	https://www.snapgene.com/
Prism 8	GraphPad Software	https://www.graphpad.com/scientific-software/prism/
ImageJ	NIH	https://imagej.nih.gov/ij/
NIS Elements Digital Imaging software	Nikon	https://www.microscope.healthcare.nikon.com/products/software/nis-elements
Leica LAS X	Leica	https://www.leica-microsystems.com/products/microscope-software/p/leica-las-x-ls/
FlowJo	FlowJo, LLC	https://www.flowjo.com/